optica

Self-phase modulation cancellation in a high-power ultrafast thin-disk laser oscillator: supplementary material

F. SALTARELLI,* A. DIEBOLD, I.J. GRAUMANN, C.R. PHILLIPS, AND U. KELLER

Institute for Quantum Electronics, ETH Zurich, 8093 Zurich, Switzerland
**Corresponding author: saltarelli@phys.ethz.ch*

Published 11 December 2018

This document provides supplementary information to "Self-phase modulation cancellation in a high-power ultrafast thin-disk laser oscillator," https://doi.org/10.1364/OPTICA.5.001603. In this supplement, we discuss in detail the efficiency of second harmonic generation in cascaded $\chi^{(2)}$ processes. We compare the different regimes from the limits of continuous wave light to very short pulses. In particular, we present an approximate analytical solution, which we used in the Letter, describing the second harmonic generation in an intermediate regime of pulse duration. Additionally, we provide all the references for the results presented in Fig. 1 of the Letter, supplementary information on the laser cavity, and details about the thermal behavior of the nonlinear crystal.

In our paper, we deploy a device based on cascaded quadratic nonlinearities (CQN) to cancel the self-phase-modulation (SPM) picked up in air. One main requirement for the design of this device was to quantify the amount of second harmonic (SH) generated and the phase shift for the fundamental wave (FW). CQN processes [1] are well understood within the framework of the pulsed coupled wave equations (CWEs). These equations can be solved numerically. Yet, a deeper theoretical understanding and analytical formulas are a powerful tool in order to know which levers to experimentally pull for optimizing the multi-dimensional processes.

Analytical solutions for the CWEs for CQN are well known in literature in the limits of very long and very short pulses [1]. The phase shift is usually approximated with Eq. (1) of the letter. We found that this equation accurately matches the numerical solution in the regime in which we operate the crystal (see Fig. 3 of the letter and related discussion). Regarding the amount of SH generated, i.e. the inverse saturable losses seen by the laser, the cascading regime often refers to a situation where the length of the crystal is long enough such that the minima of the second-harmonic-generation (SHG) process are completely smoothed out. In this regime, the SHG efficiency scales as $1/\Delta k^2$. Conversely, for longer pulses or short crystals, a $sinc^2$ tuning curve of SHG efficiency versus crystal angle is recovered, leading to very small SHG losses in the minima of this function. In our case, in order to minimize the SHG losses in the laser, we operate the crystal in a regime where these SHG efficiency minima are still pronounced. This corresponds to a regime of intermediate pulse duration between the limit of very short and long pulses. Since we could not find analytical approximations for the SHG efficiency in this regime, we developed it, see Eq. (2) of the letter. Here we present the derivation of this formula.

In the first section of this document, we introduce the formalism and the efficiency of the SHG process in the well-known case of continuous plane waves. In the second section, we switch from continuous wave (cw) to pulses and obtain an approximate solution for the losses in the SHG minima. Additionally, we discuss the different regimes and the range of validity of our analytical approximation. In section three we provide all the references used in Fig. 1 of the letter. In section four we describe in details the cavity design used in the presented laser oscillator and compare it to other possible designs. Lastly, in section five, we provide some details on the thermal behavior of the nonlinear crystal during laser operation.

1. COUPLED WAVE EQUATIONS

We start with the continuous-wave case and use the CWEs in the slowly-varying-envelope approximation (SVEA), including first-order dispersion. We consider the envelopes of the electric field E_i, where the subscript i = 1,2, corresponds, respectively, to the FW and

the SH. We define the group-velocity-mismatch (GVM) coefficient $\delta = 1/v_{g2} - 1/v_{g1}$ where v_{gi} is the group velocity. Additionally, we define the phase mismatch $\Delta k_0 = k(\omega_2) - 2k(\omega_1)$ where ω_i is the angular frequency. The other parameters entering the CWEs are the effective nonlinear coefficient for SHG d_{eff} and the index of refraction n_i.

$$\frac{\partial E_1}{\partial z} = -i\frac{\omega_1 d_{eff}}{n_1 c} E_2 E_1^* e^{-i\Delta k_0 z} \quad \textbf{(S1)}$$

$$\frac{\partial E_2}{\partial z} + \delta\frac{\partial E_2}{\partial t} = -i\frac{\omega_1 d_{eff}}{n_2 c} E_1^2 e^{i\Delta k_0 z} \quad \textbf{(S2)}$$

For further analysis, it is convenient to rewrite the CWEs in terms of a normalized electric field $\overline{E}_j$ such that its square magnitude is the intensity normalized to the input intensity of the FW, $I_{1,pk}$. Thus, we define:

$$\overline{E}_j = E_j \frac{1}{\sqrt{n_1 / n_j}\, E_{1,pk}} \quad \textbf{(S3)}$$

This translates to an intensity for the electric field:

$$I_j = \frac{n_j \varepsilon_0 c \left|E_j\right|^2}{2} = I_{1,pk}\left|\overline{E}_j\right|^2 \quad \textbf{(S4)}$$

Additionally, we define a coefficient Γ_{pk} including the properties of the nonlinear medium and the intensity of the FW as:

$$\Gamma_{pk} = \frac{\omega_1 d_{eff} E_{1,pk}}{\sqrt{n_1 n_2}\, c} \quad \textbf{(S5)}$$

In this way, we can rewrite the CWEs in (S1) and (S2) as:

$$\frac{\partial \overline{E}_2}{\partial z} + \delta\frac{\partial \overline{E}_2}{\partial t} = -i\Gamma_{pk}\overline{E}_1^2 e^{i\Delta k_0 z} \quad \textbf{(S6)}$$

$$\frac{\partial \overline{E}_1}{\partial z} = -i\Gamma_{pk}\overline{E}_2\overline{E}_1^* e^{-i\Delta k_0 z} \quad \textbf{(S7)}$$

In the approximation of low depletion of the fundamental, we solve Eq. (S7) assuming $\overline{E}_1(z) = 1$. The solution of this equation in a phase-matched condition, i.e., $\Delta k_0 = 0$ and for a nonlinear medium of length L is well known. In particular, the efficiency of the SHG process is:

$$\eta_{pk} = \left|\frac{\overline{E}_2(L)}{\overline{E}_1(0)}\right|^2 = \left(\Gamma_{pk} L\right)^2 = \left(\frac{\omega_1 d_{eff} E_{1,pk}}{\sqrt{n_1 n_2}\, c} L\right)^2 \quad \textbf{(S8)}$$

2. PULSED SECOND HARMONIC GENERATION

Next, we calculate the efficiency of the SHG process for pulses instead of cw. For this, we switch to the frequency domain, using the Fourier transform and find a propagation equation for the SH. By applying the Fourier transform operator $F_\nu[g] = \int_{-\infty}^{\infty} g(t)\exp(-2\pi i\nu t)dt$ to the left and right hand side of Eq. (S2), it becomes:

$$\frac{\partial \widetilde{E}_2}{\partial z} + i\delta(2\pi\nu)\widetilde{E}_2 = -i\Gamma_{pk}F_\nu\left[\overline{E}_1^2\right]e^{i\Delta k_0 z} \quad \textbf{(S9)}$$

where $\widetilde{E}_i$ is the normalized electric field $\overline{E}_i$ in the frequency domain and ν represents the frequency offset relative to the carrier. Without nonlinear effects, i.e. $d_{eff} = 0$, the solution of this equation is $\widetilde{E}_2 = a\exp\left(-2\pi i\delta\nu z\right)$, where a is a constant. Thus, it is convenient to search for a solution to the general equation with $d_{eff} \neq 0$ in the form $\widetilde{E}_2 = \widetilde{A}_2\exp\left(-2\pi i\delta\nu z\right)$. In our soliton modelocked TDL, the pulses have a *sech* shape in both frequency and time domain [2], thus we take a *sech* function for the electric field of the fundamental wave: $\overline{E}_1(t) = \mathrm{sech}(t/\tau)$. By using this expression for the electric field and integrating Eq. (S9) in dz from 0 to L, we again calculate the ratio between the energy in the SH at the output of the crystal and the initial energy in the FW:

$$\frac{\eta_{pw}}{\eta_{pk}} = 2\tau\int_{-\infty}^{\infty}\left|\frac{\pi^2\nu\tau}{\sinh\left(\pi^2\nu\tau\right)}\mathrm{sinc}\left(\frac{\Delta k(\nu)L}{2}\right)\right|^2 d\nu \quad \textbf{(S10)}$$

where we defined $\Delta k(\nu) = \Delta k_0 + (2\pi\nu)\delta$. The efficiency in Eq. (S10) assumes a spatial plane wave interaction, thus we called it η_{pw}. In the laser, the beam has a TEM_{00} spatial mode, that is a Gaussian profile. This corresponds to an electric field distribution of the form $E(r) \sim \exp[-(r/w)^2]$ where w is the beam radius. Hence, we need to calculate the average efficiency over this beam profile. The total energy in the FW is given by the two-dimensional spatial integral of $|E(r)|^2$. The SH is proportional to the square of the intensity of the fundamental and so the energy included in it is given by the integral of $(|E(r)|^2)^2$. By calculating the ratio between these two integrals, we get ½. Thus for a beam with a Gaussian profile, the efficiency of the SHG process $\eta = ½\ \eta_{pw}$:

$$\frac{\eta}{\eta_{pk}} = \tau\int_{-\infty}^{\infty}\left(\frac{\pi^2\nu\tau}{\sinh\left(\pi^2\nu\tau\right)}\right)^2\frac{\sin^2\left(\Delta k(\nu)L/2\right)}{(\Delta k(\nu)L/2)^2}d\nu\,. \quad \textbf{(S11)}$$

We now assume that the bandwidth of the pulse is narrow enough such that the denominator $\Delta k(\nu)L/2$ does not change significantly before the $\sinh(\pi^2\nu\tau)$ brings the integrand to zero. Thus, we approximate $\Delta k(\nu)$ in the denominator with its value at the carrier wavelength, i.e. Δk_0. Additionally, we assume that the center wavelength corresponds to a SHG minimum, i.e. $\sin(\Delta k_0 L/2) = 0$. It should be noted that this assumption will reduce our final resulting formula to the case of operation in the SHG minima only. Using the definition of $\Delta k(\nu)$ we have that, in this condition $\sin^2(\Delta k(\nu)L/2) = \sin^2[(2\pi\nu)\delta L/2]$. We can thus approximate Eq. (S11) as:

$$\frac{\eta}{\eta_{pk}} = \frac{4\tau}{\left(\Delta k_0 L\right)^2}\int_{-\infty}^{\infty}\left(\frac{\pi^2\nu\tau}{\sinh\left(\pi^2\nu\tau\right)}\right)^2\sin\left(\frac{2\pi\nu\delta L}{2}\right)^2 d\nu\,. \quad \textbf{(S12)}$$

This integral can be solved analytically and yields:

$$\frac{\eta}{\eta_{pk}} = \frac{2}{3\left(\Delta k_0 L\right)^2}\left[1 + \frac{\left(3 - 3\overline{\delta}\coth\left(\overline{\delta}\right)\right)}{\sinh\left(\overline{\delta}\right)^2}\right], \quad \textbf{(S13)}$$

where $\overline{\delta} = \delta L/\tau$ is the ratio between the temporal walk-off between the FW and the SH in the crystal δL and the *sech*-pulse

duration parameter τ. For the sake of clarity we want to stress again that Eq. (S12) and (S13) hold only in the SHG minima, that is for $\Delta k_0 L = 2\pi n_{min}$. As a function of the parameter $\bar{\delta}$, the solution of Eq. (S13) is shown in Fig. S1 in units of $2/[3(\Delta k_0 L)^2]$ in blue.

First we discuss the two limits for $\bar{\delta}$, namely $\bar{\delta} = 0$ and $\bar{\delta} >> 1$. In the limit of large $\bar{\delta}$ that is a large GVM compared to the pulse duration, as we see in Fig. S1 the expression in square brackets in (S13) is 1, which implies:

$$\frac{\eta}{\eta_{pk}} = \frac{2}{3(\Delta k_0 L)^2} \quad \left(\bar{\delta} >> 1\right) \tag{S14}$$

This is a well-known result in the context of CQN [3,4]. The opposite limit is $\bar{\delta} = 0$, which corresponds to the case of negligible temporal walk off relative to the pulse duration (i.e. narrow bandwidths or short crystals). This results in no SHG in the SHG minima.

In our experiments we operate with a relatively small value of $\bar{\delta}$, in order to minimize the SHG losses. In the time domain this corresponds to a situation where the temporal walk off between the FW and the SH is a small fraction of the pulse duration. In the frequency domain, this corresponds to a pulse whose spectrum is narrow enough such that $\Delta k(\lambda)$ is close to $2\pi n_{min}$ across the whole pulse spectrum. Thus, we carry out a second-order Taylor expansion of Eq. (S13) around $\bar{\delta} = 0$ obtaining:

$$\frac{\eta}{\eta_{pk}} \approx \frac{4}{15}\left(\frac{\delta}{\Delta k_0 \tau}\right)^2 \tag{S15}$$

This solution corresponds to the red curve in Fig. S1 and it differs for less than 10% from the value of Eq. (S13) for $|\bar{\delta}| < 0.7$. In terms of full-width-at-half-maximum (FWHM) pulse duration $\tau_p = 1.76\tau$, $|\bar{\delta}| < 0.7$ corresponds to: $\delta L / \tau_p < 0.4$. For the nonlinear crystal used in this laser experiment, the temporal walk off in the L=5-mm LBO crystal corresponds to 270 fs. Thus Eq. (S15) is correct within 10% if τ_p > 700 fs. This was indeed the case for our laser experiments.

By defining a new constant:

$$\xi = \frac{2\omega_1^2 d_{eff}^2}{n_1^2 n_2 c^3 \varepsilon_0} \tag{S16}$$

we rewrite Eq. (S15) in the form presented in the letter in Eq. 2:

$$\eta \approx 0.83\xi\left(\frac{\delta L}{\Delta k_0 \tau_p}\right)^2 I_{1,pk} \tag{S17}$$

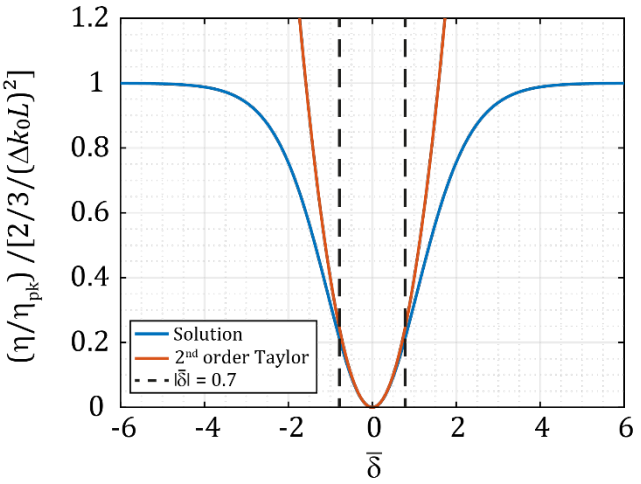

Fig. S1 Calculated value of Eq. (S13) and second-order Taylor expansion. The variable on the *x* axis $\bar{\delta} = \delta L / \tau$ is the ratio between the temporal walk off in the crystal between FW and SH and the *sech* pulse duration parameter τ. In the area within the vertical dashed lines, the Taylor expansion differs for less than 10% from the exact solution.

3. OVERVIEW OF STATE-OF-THE-ART THIN-DISK OSCILLATORS

In Fig. S2, we reproduce Fig. 1 of the letter, including a full list of citations for the data points.

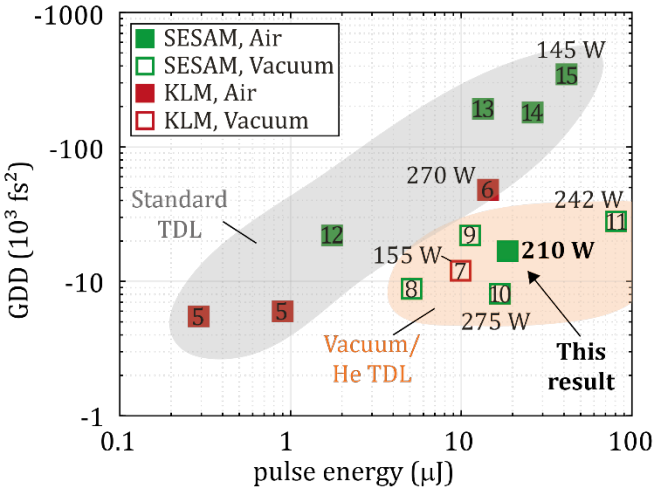

Fig. S2 State-of-the-art thin-disk oscillators. Overview of their performance in terms of introduced round-trip group delay dispersion (GDD) versus output pulse energy. The number in the symbol gives the reference [5-15].

4. CAVITY DESIGN

In this section, we provide additional details on the resonator cavity, which includes three reflections on the disk gain medium. The $1/e^2$ beam radius as a function of the position inside the cavity is shown in Fig. S3 as it is obtained by standard ABCD matrix calculations. The cold disk radius of curvature (ROC) is R_{cold} = 2.04 m. During laser operation, because of thermal lensing the disk's curvature changes. Here we estimated a $F_{disk} = 2/R_{lasing} - 2/R_{cold}$ = -0.035/m [16]. We have the SESAM at position 0 and the output coupler (OC) at the other end of the cavity. In order to have multiple passes on the disk we implemented a relay-imaging active multi-pass architecture [13]. In this way by properly spacing the two concave mirrors (ROC = 2.0 m) and the disk, we obtain the same Gaussian beam radius and

curvature for each pass on the disk. This arrangement helps minimize the misalignment sensitivity of our cavity design. This is defined as the displacement of the laser beam on the disk because of an angular misalignment of the disk itself. This plays an important role for thin-disk lasers operated in air since a gas-wedge effect due to the air heating up in front of the disk leads to potential instabilities [16, 17]. Additionally, this configuration allows us to use different spots on the same mirrors in order to increase the number of passes on the disk. In this way, a very small angle of incidence (AOI) (<3 deg) is possible on the disk and on the curved mirrors. This minimizes astigmatism, which is detrimental for modelocked operation.

All the mirrors in our cavity are manufactured by Layertec GmbH except for the two high-dispersive (HD) flat mirrors providing -2'000 fs² of GDD each, which are made by University of Neuchatel. The curved dispersive mirrors provide -550 fs² of GDD per bounce. The thin film polarizer (TFP), also provided by Layertec GmbH, yields ≈ -550 fs² of GDD per bounce.

The total SPM picked up in air is calculated as the B integral according to the formula:

$$B_{air,rt} = \frac{2\pi}{\lambda}\frac{2T_{OC}}{\log(1/R_{OC})}P_{pk,IC}\left(\int_0^l \frac{n_{2,air}}{\pi w^2(z)/2}dz\right) \quad \textbf{(S18)}$$

where λ is the wavelength, T_{OC} and R_{OC}, respectively, the transmission and the reflectivity of the OC, P_{pkIC} the intracavity peak power immediately before the OC, l the length of the cavity, $w(z)$ the beam radius inside the laser cavity, and $n_{2,air} = 4 \times 10^{-19}$ cm²/W [18] the nonlinear refractive index of air. The factor $2T_{OC}/\log(1/R_{OC})$ takes into account that the peak intensity is not constant in a round trip and assumes an exponential growth [19].

Some TDLs use an alternative approach based on convex mirrors to obtain a design having less intracavity foci [16, 17, 20]. While the reduced number of foci results in a lower amount of SPM picked up in air, such cavities are not compatible with the multi-pass architecture we use here. Therefore, they exhibit increased misalignment sensitivity. These issues motivated our use of the cavity design shown in Fig. S3.

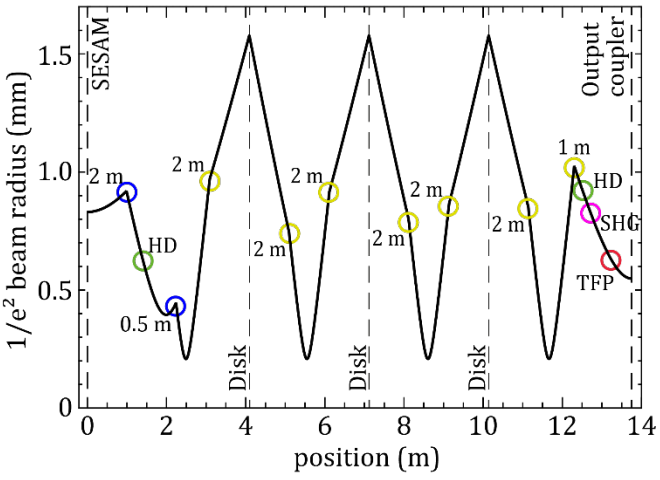

Fig. S3 Evolution of the $1/e^2$ beam radius. Vertical dashed lines indicate the position, respectively, of the SESAM, the disk and the output coupler. We report the position of the curved mirrors, the dispersive mirrors, the thin-film polarizer (TFP), and the SHG crystal with circles. Blue circles refer to curved high-reflectivity mirrors, yellow circles to dispersive mirrors providing -550 fs² GDD, green circles to flat high-dispersive (HD) mirrors providing -2'000 fs² GDD. The numbers in the Figure refer to the radius of curvature of concave mirrors.

5. THERMAL BEHAVIOR OF THE NONLINEAR CRYSTAL

Using a calibrated thermal camera (FLIR SC640), we measured the temperature of the SHG crystal during laser operation. We record a temperature increase in the steady state of ≈ 10 °C at the highest output power (210 W average output power, with more than 500 W of intracavity power). This implies a low absorption from the crystal since no control over the crystal temperature was in place. Therefore, we expect that this SPM-cancellation technique is suitable for laser operation toward the kW output-power level [21]. The time needed by the nonlinear crystal to reach thermal equilibrium was in the order of a minute. During this transient phase, the laser stayed modelocked.

References

1. F. Wise, L. Qian, and X. Liu, "Applications of cascaded quadratic nonlinearities to femtosecond pulse generation," Journal of Nonlinear Optical Physics & Materials **11**, 317-338 (2002).
2. F. X. Kärtner, I. D. Jung, and U. Keller, "Soliton Mode-Locking with Saturable Absorbers," IEEE J. Sel. Top. Quant. **2**, 540-556 (1996).
3. G. I. Stegeman, D. J. Hagan, and L. Torner, "χ(2) cascading phenomena and their applications to all-optical signal processing, mode-locking, pulse compression and solitons," Optical and Quantum Electronics **28**, 1691-1740 (1996).
4. C. R. Phillips, A. S. Mayer, A. Klenner, and U. Keller, "SESAM modelocked Yb:CaGdAlO4 laser in the soliton modelocking regime with positive intracavity dispersion," Opt. Express. **22**, 6060-6077 (2014).
5. J. Zhang, J. Brons, N. Lilienfei, E. Fedulova, V. Pervak, D. Bauer, D. Sutter, Z. Wei, A. Apolonski, O. Pronin, and F. Krausz, "260-megahertz, megawatt-level thin-disk oscillator," Optics Letters **40**, 1627-1630 (2015).
6. J. Brons, V. Pervak, E. Fedulova, D. Bauer, D. Sutter, V. Kalashnikov, A. Apolonskiy, O. Pronin, and F. Krausz, "Energy scaling of Kerr-lens mode-locked thin-disk oscillators," Opt. Lett. **39**, 6442-6445 (2014).
7. J. Brons, V. Pervak, D. Bauer, D. Sutter, O. Pronin, and F. Krausz, "Powerful 100-fs-scale Kerr-lens mode-locked thin-disk oscillator," Opt. Lett. **41**, 3567-3570 (2016).
8. S. V. Marchese, T. Südmeyer, M. Golling, R. Grange, and U. Keller, "Pulse energy scaling to 5 μJ from a femtosecond thin disk laser," Opt. Lett. **31**, 2728-2730 (2006).
9. S. V. Marchese, C. R. E. Baer, A. G. Engqvist, S. Hashimoto, D. J. H. C. Maas, M. Golling, T. Südmeyer, and U. Keller, "Femtosecond thin disk laser oscillator with pulse energy beyond the 10-microjoule level," Opt. Express **16**, 6397-6407 (2008).
10. C. J. Saraceno, F. Emaury, O. H. Heckl, C. R. E. Baer, M. Hoffmann, C. Schriber, M. Golling, T. Südmeyer, and U. Keller, "275 W average output power from a femtosecond thin disk oscillator operated in a vacuum environment," Opt. Express **20**, 23535-23541 (2012).
11. C. J. Saraceno, F. Emaury, C. Schriber, M. Hoffmann, M. Golling, T. Südmeyer, and U. Keller, "Ultrafast thin-disk laser with 80 μJ pulse energy and 242 W of average power," Opt. Lett. **39**, 9-12 (2014).
12. E. Innerhofer, T. Südmeyer, F. Brunner, R. Häring, A. Aschwanden, R. Paschotta, U. Keller, C. Hönninger, and M. Kumkar, "60 W average power in 810-fs pulses from a thin-disk Yb:YAG laser," Opt. Lett. **28**, 367-369 (2003).
13. J. Neuhaus, J. Kleinbauer, A. Killi, S. Weiler, D. Sutter, and T. Dekorsy, "Passively mode-locked Yb:YAG thin-disk laser with pulse energies exceeding 13 μJ by use of an active multipass geometry," Opt. Lett. **33**, 726-728 (2008).
14. J. Neuhaus, D. Bauer, J. Zhang, A. Killi, J. Kleinbauer, M. Kumkar, S. Weiler, M. Guina, D. H. Sutter, and T. Dekorsy, "Subpicosecond thin-disk laser oscillator with pulse energies of up to 25.9 microjoules by use of an active multipass geometry," Opt. Express **16**, 20530-20539 (2008).
15. D. Bauer, I. Zawischa, D. H. Sutter, A. Killi, and T. Dekorsy, "Mode-locked Yb:YAG thin-disk oscillator with 41 μJ pulse energy at 145 W average infrared power and high power frequency conversion," Opt. Express **20**, 9698-9704 (2012).
16. A. Diebold, F. Saltarelli, I. J. Graumann, C. J. Saraceno, C. R. Phillips, and U. Keller, "Gas-lens effect in kW-class thin-disk lasers," Opt. Express. **26**, 12648-12659 (2018).

17. T. Dietrich, S. Piehler, C. Roecker, M. Rumpel, M. A. Ahmed, and T. Graf, "Passive compensation of the misalignment instability caused by air convection in thin-disk lasers," Opt. Lett. **42**, 3263-3266 (2017).
18. E. T. J. Nibbering, G. Grillon, M. A. Franco, B. S. Prade, and A. Mysyrowicz, "Determination of the inertial contribution to the nonlinear refractive index of air, N_2, and O_2 by use of unfocused high-intensity femtosecond laser pulses," J. Opt. Soc. Am. B **14**, 650-660 (1997).
19. J. Neuhaus, D. Bauer, J. Kleinbauer, A. Killi, D. H. Sutter, and T. Dekorsy, "Numerical analysis of a sub-picosecond thin-disk laser oscillator with active multipass geometry showing a variation of pulse duration within one round trip," Journal of the Optical Society of America B **27**, 65-71 (2010).
20. K. Schuhmann, K. Kirch, and A. Antognini, "Multi-pass oscillator layout for high-energy mode-locked thin-disk lasers," ArXiv, 1603.00404v00402 (2016).
21. T. Dietrich, S. Piehler, M. Rumpel, P. Villeval, D. Lupinski, M. Abdou-Ahmed, and T. Graf, "Highly-efficient continuous-wave intra-cavity frequency-doubled Yb:LuAG thin-disk laser with 1 kW of output power," Opt. Express. **25**, 4917-4925 (2017).